ISSN: 2278-4632
Vol-13, Issue-02, No.01, February 2023

FLC-MPC based Direct Torque Control for Matrix Converter-Fed Induction Motor Drive

PUJARI SREEHARI, PG-Scholar, Department of EEE, JNTUA COLLEGE OF ENGINEERING ANANTHAPURAM, India.
Dr.M.ANKA RAO Assistant Professor, Department of EEE, , JNTUA COLLEGE OF ENGINEERING ANANTHAPURAM,
pjrsreehari9@gmail.com[1], ankaraomogili@gmail.com[2],

Abstract
In this research, a model predictive control (MPC) with fuzzy logic controller based DTC approach for a direct matrix converter-fed induction motor is given. This method aims to eliminate the torque ripple in motors caused by the usage of model predictive control (MPC)-based DTC. These are obtained from the electromagnetic torque and stator flux control employing all possible voltage vectors and their corresponding switching states. The best switching state that minimises the cost function associated to the electromagnetic torque has then been chosen using the Finite Control Set Model Predictive Control (FCS-MPC). In the proposed method, evaluate the total hormonic distortion comparison between PI controller and fuzzy logic controller. To evaluate the performance of the proposed method, evaluate the results by using Matlab and Simulink software.

Index Terms—Direct torque control, finite control set model predictive control, induction motor, matrix converter, fuzzy logic controller

I INRODUCTION
Due to its inherent benefits, such as bidirectional energy flow, variable input power factor, the possibility for high power density, and the absence of large dc-link capacitors, MATRIX converter (MC) has received a lot of attention [1-4]. Previous research has mostly focused on the MC's modulation and switching pattern [5]–[6].
Less research has been done on high-performance speed control for MC-fed induction motors (IM). Casadei made the initial suggestion for the direct torque control (DTC) approach for MC-fed IM [7], which was later experimentally confirmed [8]. However, the main limitations have been recognised as variable frequency operation, torque ripple, and flux ripple [9].
To solve these issues, a number of techniques based on switching tables and constant switching frequency [10, 11] imposed in DTC have been used. It was suggested in [10] to employ the space vector approach, a flux dead-beat algorithm, and direct torque control to reduce torque ripple and achieve unity input power factor. A better DTC technique is suggested in [11], which is based on twelve 30° voltage and flux vector sectors for MC-fed IM. The best switching vector was chosen using a new lookup table to regulate the torque with the fewest fluctuations in stator flux within the hysteresis band. Because of this, a lower torque ripple was obtained than with the traditional DTC approach, but the necessary look-up table is complicated. Due to the FCS-advantages, MPC's including its quick dynamic response, simplicity in including nonlinearities and system restrictions, and adaptability in incorporating additional system requirements, it has been developed and applied to the control of power converters and motor drives [12]–[16]. For a 2-level voltage source inverter-fed induction motor drive, an improved model predictive torque control is proposed in [17] that lowers control complexity and torque ripple.
A weighting factor optimization technique is provided in [18] for lowering the torque ripple of induction machines fed by indirect matrix converters. Using MPC to regulate the stator current, a predictive current control approach for an IM based on the MC was developed in [19], which also controls the torque and flux of the IM. The cost function, which takes a while, uses all 27 legitimate switching states. MPC is used in [20] to regulate the stator flux and electromagnetic torque.
However, it continues to take into account each of the 27 switching states, leaving the issue of time-consuming calculations unresolved.
The calculation effort for the MC using the FCS-MPC approach has been reduced using a number of methods [21]–[22].
In this research, an improved MPC-based DTC strategy for a direct matrix converter-fed (DMC-fed) IM is developed in order to eliminate the torque ripple induced by traditional DTC method.

ISSN: 2278-4632
Vol-13, Issue-02, No.01, February 2023

According to the idea of direct torque control, the suggested approach directly controls electromagnetic torque and stator flux to produce the desired control effect.
In order to properly utilise the available switching states, two look-up tables are suggested. Nine switching states are already chosen in accordance with the two look-up tables, saving a significant amount of processing time.

$$\begin{bmatrix} v_{oa} \\ v_{ob} \\ v_{oc} \end{bmatrix} = \begin{bmatrix} S_{Aa} & S_{Ab} & S_{Ac} \\ S_{Ba} & S_{Bb} & S_{Bc} \\ S_{Ca} & S_{Cb} & S_{Cc} \end{bmatrix} \begin{bmatrix} v_{ia} \\ v_{ib} \\ v_{ic} \end{bmatrix} \quad (1)$$

The ideal switching state for the subsequent control period is then chosen using MPC. The proposed MPC-based DTC for MC-fed IM has certain principles that are presented in [23].

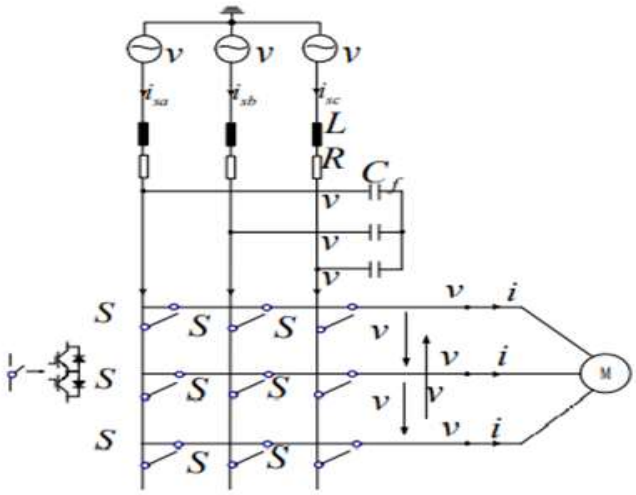

Fig. 1. Topology of direct matrix converter

To overcome the drawbacks of existing MPC based DTC this article proposes a FLC-MPC based Direct Torque Control for Matrix Converter-Fed Induction Motor with Reduced Torque Ripple. The rest of the article arranged as follows, the system description and its control method are presented in Section II, and the proposed method and implementation is given in detail in Section III. The simulation results verified in Section IV. Finally, Section V concludes this article.

II SYSTEM DISCRIPTION

There are nine bidirectional switches in the DMC, as shown in Fig. 1, and each one of them is there to make sure that bi-directional energy flow occurs. The input filter, which is connected between the grid and the converter, tries to reduce high harmonic distortion in the grid current. The mathematical representation of the DMC's input and output can be expressed as follows in accordance with its topology:

$$\begin{bmatrix} i_{ia} \\ i_{ib} \\ \cdot \end{bmatrix} = \begin{bmatrix} S_{Aa} & S_{Ab} & S_{Ac} \\ S_{Ba} & S_{Bb} & S_{Bc} \\ \cdot & \cdot & \cdot \end{bmatrix}^T \begin{bmatrix} i_{oa} \\ i_{ob} \\ i_{oc} \end{bmatrix} \quad (2)$$

$$S = \begin{bmatrix} S_{Aa} & S_{Ab} & S_{Ac} \\ S_{Ba} & S_{Bb} & S_{Bc} \\ S_{Ca} & S_{Cb} & S_{Cc} \end{bmatrix} \quad (3)$$

Where the output voltage and filter capacitor voltage are represented by ol v (l a b c,,,), and ij v (j a b c,,,), respectively. The output current and input current are represented by ol I and ij i. Nine bidirectional switches that satisfy the following equation are represented by Xy S (X A B C,,,, y A B C,,):

ISSN: 2278-4632
Vol-13, Issue-02, No.01, February 2023

$$S_{Xy}=\begin{cases}1 & S_{Xy}\ \text{is on}\\ 0 & S_{Xy}\ \text{is off}\end{cases} \quad (4)$$

Taking into account the DMC's prohibitions: (1) No open circuit at the DMC's output; (2) No short circuit at the DMC's input. As a result, the following equation must be true:

$$\begin{cases}S_{Aa}+S_{Ab}+S_{Ac}=1\\ S_{Ba}+S_{Bb}+S_{Bc}=1\\ S_{Ca}+S_{Cb}+S_{Cc}=1\end{cases} \quad (5)$$

DMC has 27 valid switching states, and Table I lists each switching state along with its output voltage and input current. All switching states can be categorised into one of three groups:

TABLE I : SPACE VECTORS OF DMC

Categories	Switching states	A B C				
I	+1	a b b	$2/3\ v_{dc}$	0	$2/\sqrt{3}i_{dc}$	$-\pi/6$
I	-1	b a a	$-2/3\ v_{dc}$	0	$-2/\sqrt{3}i_{dc}$	$-\pi/6$
I	+2	b c c	$2/3\ v_{dc}$	0	$2/\sqrt{3}i_{dc}$	$\pi/2$
I	-2	c b b	$-2/3\ v_{dc}$	0	$-2/\sqrt{3}i_{dc}$	$\pi/2$
I	+3	c a a	$2/3\ v_{dc}$	0	$2/\sqrt{3}i_{dc}$	$7\pi/6$
I	-3	a c c	$-2/3\ v_{dc}$	0	$-2/\sqrt{3}i_{dc}$	$7\pi/6$
I	+4	b a b	$2/3\ v_{dc}$	$2\pi/3$	$2/\sqrt{3}i_{dc}$	$-\pi/6$
I	-4	a b a	$-2/3\ v_{dc}$	$2\pi/3$	$-2/\sqrt{3}i_{dc}$	$-\pi/6$
I	+5	a b c	$2/3\ v_{dc}$	$2\pi/3$	$2/\sqrt{3}i_{dc}$	$\pi/2$
I	-5	b c b	$-2/3\ v_{dc}$	$2\pi/3$	$-2/\sqrt{3}i_{dc}$	$\pi/2$
I	+6	a c a	$2/3\ v_{dc}$	$2\pi/3$	$2/\sqrt{3}i_{dc}$	$7\pi/6$
I	-6	c a c	$-2/3\ v_{dc}$	$2\pi/3$	$-2/\sqrt{3}i_{dc}$	$7\pi/6$
I	+7	b b a	$2/3\ v_{dc}$	$4\pi/3$	$2/\sqrt{3}i_{dc}$	$-\pi/6$
I	-7	a a b	$-2/3\ v_{dc}$	$4\pi/3$	$-2/\sqrt{3}i_{dc}$	$-\pi/6$
I	+8	c c b	$2/3\ v_{dc}$	$4\pi/3$	$2/\sqrt{3}i_{dc}$	$\pi/2$
I	-8	b b c	$-2/3\ v_{dc}$	$4\pi/3$	$-2/\sqrt{3}i_{dc}$	$\pi/2$
I	+9	a a c	$2/3\ v_{dc}$	$4\pi/3$	$2/\sqrt{3}i_{dc}$	$7\pi/6$
I	-9	c c a	$-2/3\ v_{dc}$	$4\pi/3$	$-2/\sqrt{3}i_{dc}$	$7\pi/6$
II	0	a a a	0	—	0	—
II	0	b b b	0	—	0	—
II	0	c c c	0	—	0	—
III	—	a b c	v_{om}	α_o	i_{im}	β_i
III	—	a c b	$-v_{om}$	$-\alpha_o$	i_{im}	$-\beta_i$
III	—	b a c	$-v_{om}$	$-\alpha_o+4\pi/3$	i_{im}	$-\beta_i+2\pi/3$
III	—	b c a	v_{om}	$\alpha_o+4\pi/3$	i_{im}	$\beta_i+2\pi/3$
III	—	c a b	v_{om}	$\alpha_o+2\pi/3$	i_{im}	$\beta_i+4\pi/3$
III	—	c b a	$-v_{om}$	$-\alpha_o+2\pi/3$	i_{im}	$-\beta_i+4\pi/3$

Category I: Known as "active vectors," each switching state can produce space vectors with a fixed direction and variable amplitude. Category II: "Zero vectors" are space vectors with zero amplitude and changeable direction. Category III: In this category, the space vectors produced by the switching states have a variable direction but a fixed amplitude. These vectors are referred to as "spinning vectors."

The active voltage vector can fall into six directions in the -plane, as illustrated in Fig. 2a, because each active vector (category I) has a definite direction. The input current vector ii and output voltage vector vo can be written as:

$$\boldsymbol{v}_o=\frac{2}{3}(v_{oa}+v_{ob}e^{j(2\pi/3)}+v_{oc}e^{j(4\pi/3)})=v_{om}e^{j\alpha_o} \quad (6)$$

$$\boldsymbol{i}_i=\frac{2}{3}(i_{ia}+i_{ib}e^{j(2\pi/3)}+i_{ic}e^{j(4\pi/3)})=i_{im}e^{j\beta_i} \quad (7)$$

Where V_{om} and I_{im} stand for the corresponding amplitudes of V_0 and I_i. The angles of o v and I I are represented, respectively, by o and i. The same procedure may be used to produce the source voltage vector, V_{sa}, V_{sb}, V_{sc} source current vector I_{sa}, I_{sb}, I_{sc}, and output current vector I_{oa}, I_{ob}, I_{oc}, The following is the state-space description that is obtained using the mathematical model of the input filter:

ISSN: 2278-4632
Vol-13, Issue-02, No.01, February 2023

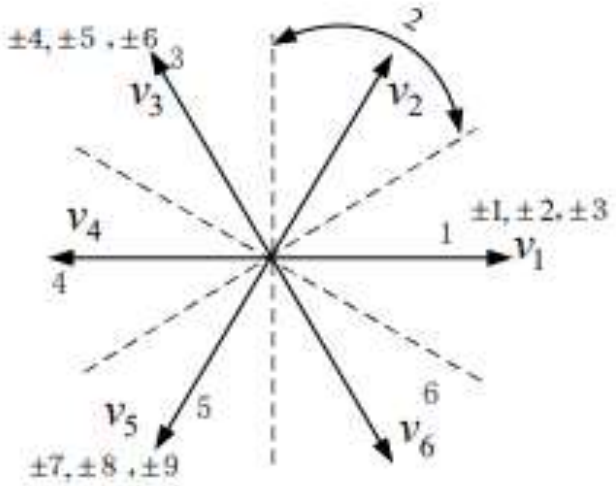

Input voltage vector

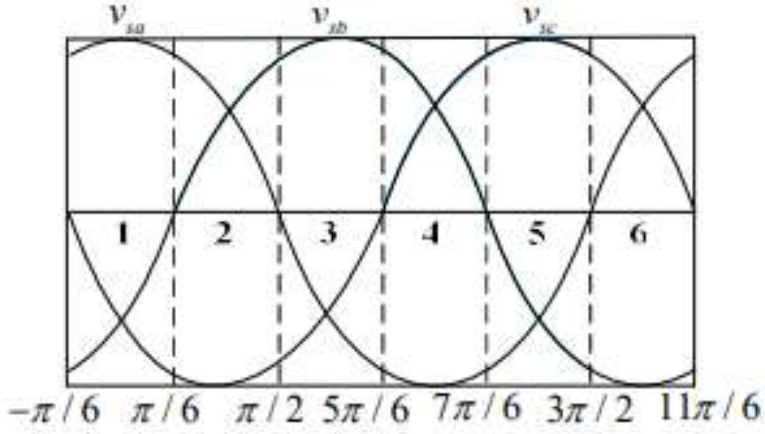

Voltage sector division

$$\begin{bmatrix} \frac{dv_i}{dt} \\ \frac{di_s}{dt} \end{bmatrix} = N \begin{bmatrix} v_i \\ i_s \end{bmatrix} + M \begin{bmatrix} v_s \\ i_i \end{bmatrix} \quad (8)$$

When N and M are matrices that have the following expressions:

$$N = \begin{bmatrix} 0 & 1/C_f \\ -1/L_f & -R_i/L_f \end{bmatrix}, M = \begin{bmatrix} 0 & -1/C_f \\ 1/L_f & 0 \end{bmatrix} \quad (9)$$

Where R_i is a passive damping resistor and C f is the filter capacitor. L f is the filter inductance. The six sectors Sn (n=1–6) that make up the - axis among those vectors (v1–v6) should each have a range that satisfies the following equation:

$$(2n-3)\pi/6 \le s_n \le (2n\text{-}1)\pi/6 \quad (10)$$

Every two switching states can produce voltage vectors that have the same direction, taking into account the sector where the input voltage is placed. As shown in Fig. 2(b), for instance, assuming that the input voltage is placed in sector 1, the switching states +1 and -3 can provide an output voltage whose direction is the same as that of v1, since the direction of v_{sac} is not fixed, $v_{sac} > 0$, and $v_{sab} > 0$. As a result, Table II explains how the DTC method's voltage vector and switching states in various voltage sectors relate to one another.

ISSN: 2278-4632
Vol-13, Issue-02, No.01, February 2023

Voltage vector	Voltage Sector					
	1	2	3	4	5	6
$\overline{v_1}$	-3, +1	+2, -3	-1, +2	+3, -1	-2, +3	+1, -2
$\overline{v_2}$	+9, -7	-8, +9	+7, -8	-9, +7	+8, -9	-7, +8
$\overline{v_3}$	-6, +4	+5, -6	-4, +5	+6, -4	-5, +6	+4, -5
$\overline{v_4}$	+3, -1	-2, +3	+1, -2	-3, +1	+2, -3	-1, +2
$\overline{v_5}$	-9, +7	+8, -9	-7, +8	+9, -7	-8, +9	+7, -8
$\overline{v_6}$	+6, ,-4	-5, +6	+4, -5	-6, +4	+5, -6	-4, +5

III PROPOSED METHOD

Fuzzy logic controllers are used in a variety of renewable energy applications (FLC). Because of its ease of use, FLC has gained in popularity over the previous decade. FLC also handles bad input, removing the requirement for the controller to use a precise mathematical model. In order to acquire the greatest power from PV modules, FLC can simply manage nonlinearity problems. It can function in any weather, with any temperature or irradiance variation.

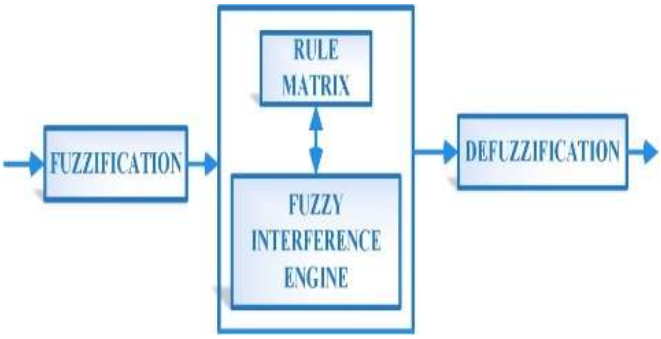

Fig.2. the Stages of Fuzzy Logic controller

There are three types of fuzzy logic controller processes:

- Fuzzification
- Rule Evaluation
- Defuzzification

The first form of Fuzzification allows crisp input, such as fluctuations in input voltage values. It uses the stored membership function to convert Crisp Input to Fuzzy Input. When the fuzzy values are designed, the first stage of FLC, Fuzzification, occurs.

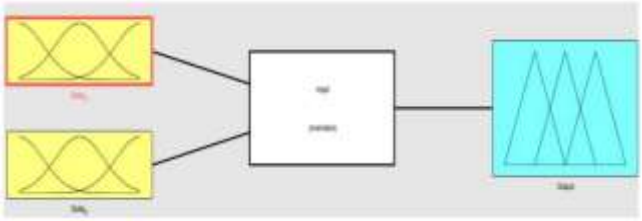

Fig.3. the FLC

The second type of Fuzzy logic controller is rule evaluation. During rule evaluation, the fuzzy processor is utilised to determine the controlling action that occurs during the response delivered to the set of input values. The Rule Evaluation gives a fuzzy output for each action. The last category in the fuzzy logic controller process is the Defuzzification Technique. The fuzzy value is turned to a crisp value during defuzzification. The crisp value from the fuzzy set is always the intended value of the output. Each fuzzy output variable in relation to the output membership function for each input set is effectively modified by the FLC Process. The centre of gravity (COG) methodology, often known as the centroid method, is the most commonly used defuzzification procedure. The Fuzzy logic controller is employed in the MPPT controller in this project, which is related to the P&O algorithm. FLC involvement in MPPT increases output voltage, and creating a Fuzzy Logic Controller that does not require much awareness of the model's specific requirements is relatively straightforward. The rule must only be assigned to each set of the membership function.

ISSN: 2278-4632
Vol-13, Issue-02, No.01, February 2023

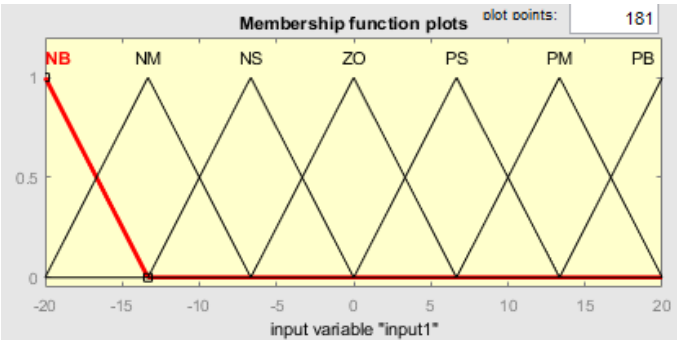

Fig.4. Speed error

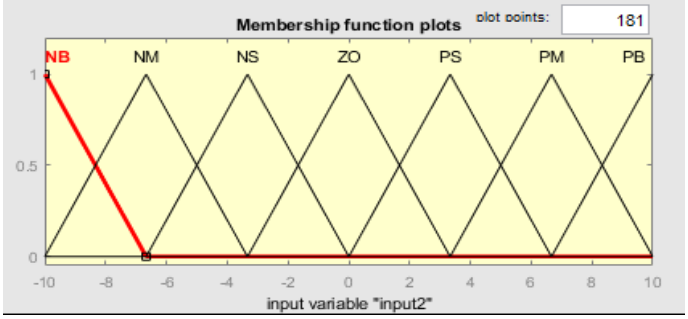

Fig.5. Change in speed error

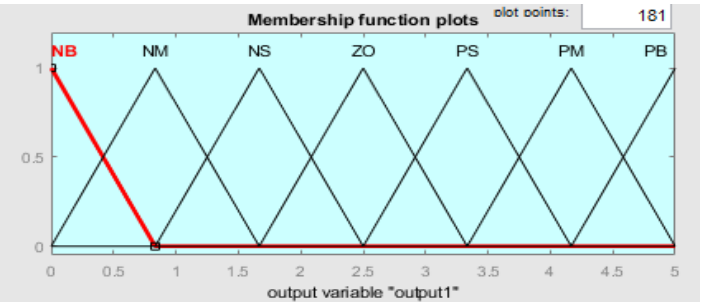

Fig.6. Reference torque

TABLE-2: Rules Table

C/CE	NB	NM	NS	ZO	PS	PM	PB
NB	PB	PB	PB	PB	PM	PS	ZO
NM	PB	PB	PM	PM	PS	ZO	ZO
NS	PB	PM	PM	PS	ZO	ZO	NS
ZO	PM	PS	PS	ZO	NS	NS	NM
PS	PS	ZO	ZO	NS	NM	NM	NB
PM	ZO	ZO	NS	NM	NM	NB	NB
PB	ZO	NS	NM	NB	NB	NB	NB

This paper introduces a novel method for constructing an MPPT for a PV module under unknown conditions. After implementing this method, the fluctuation around the Maximum PowerPoint is decreased. This technique outperforms the straightforward P&O algorithm Approach. Variations in PV module voltage (Delta V) and changes in PV module power are sent into the Fuzzy logic controller (Delta P). The fuzzy logic controller's

ISSN: 2278-4632
Vol-13, Issue-02, No.01, February 2023

output is delta Y. The fuzzy logic controller's output is delta Y. The output of the Fuzzy logic controller is fed into the sampling signal, which is altered and sent to the boost converter, which provides the switching pulses.

IV FLC SIMULATION RESULTS

IV.I Simulation results using MPC-fuzzy logic controller:

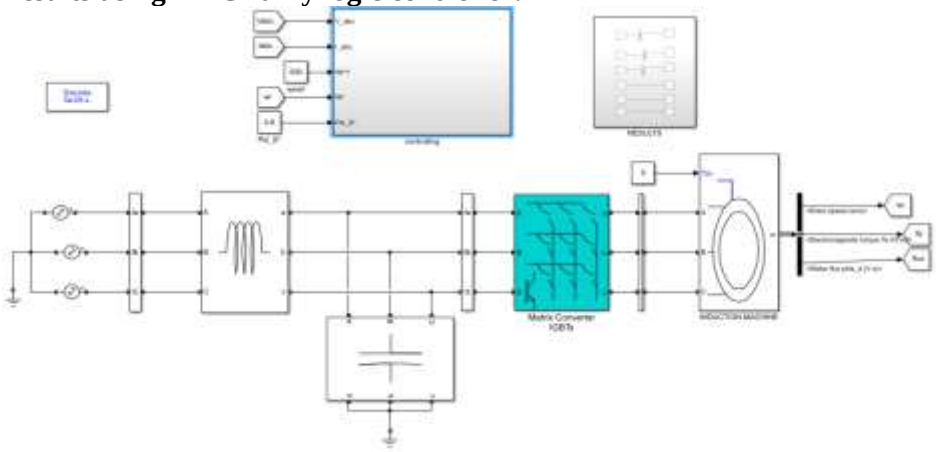

FIG.7.Schematic diagram

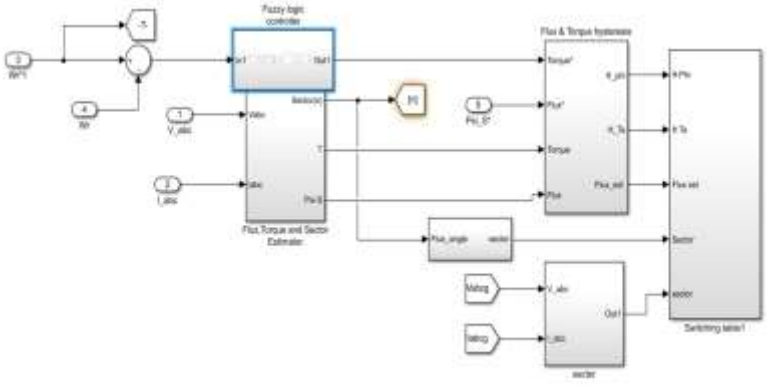

FIG.8.Controlling part

Case-1 load torque 0 N.M

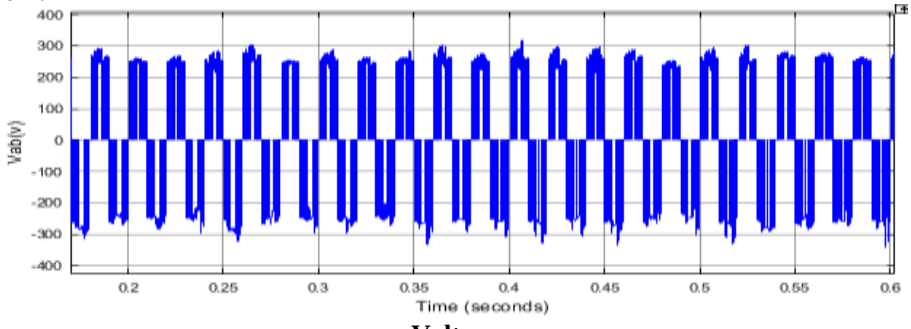

Voltage

ISSN: 2278-4632
Vol-13, Issue-02, No.01, February 2023

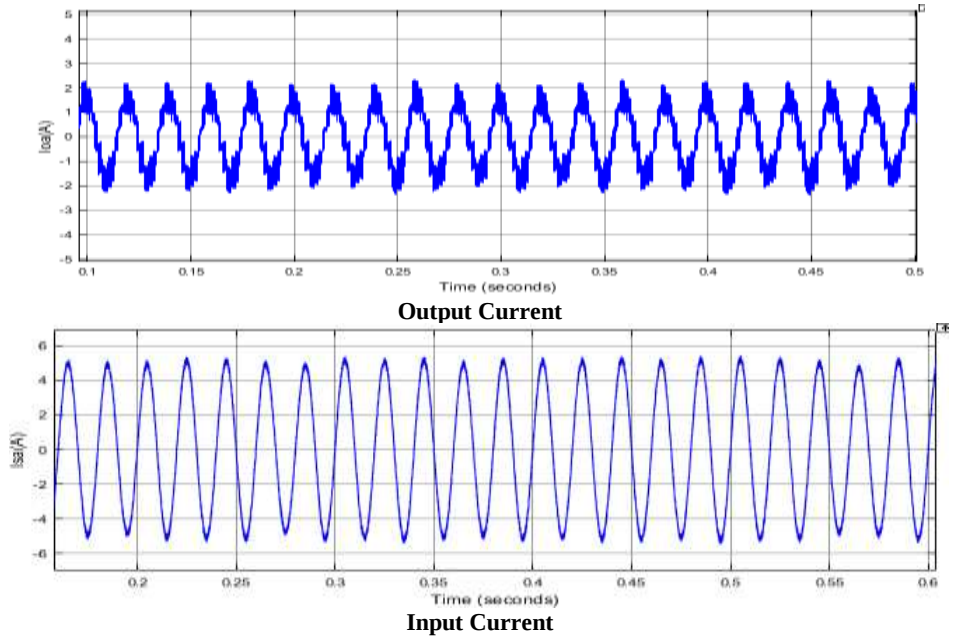

Fig. 9. Input and output waveforms of DMC with load torque equal to 0 (N.m) under the proposed MPC-based DTC method

Using the conventional DTC method and the suggested method, respectively, Figs. 9a and 9b show the waveforms of the stator voltage, stator current of the IM, and grid current. In both cases, the load torque is set at 0 Nm, the stator flux reference is equal to 0.8 Wb, and the speed reference is 600 r/min. Both approaches provide input and output current that is almost sinusoidal.

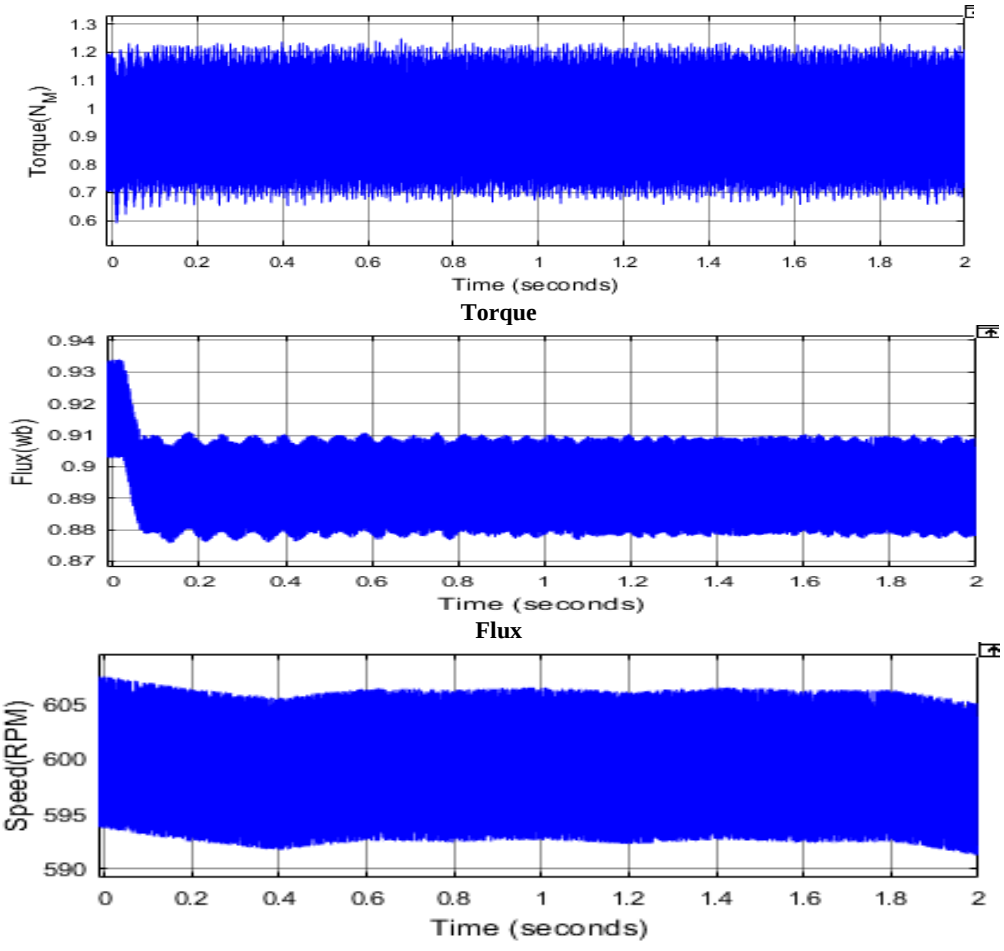

ISSN: 2278-4632
Vol-13, Issue-02, No.01, February 2023

Speed

Fig. 10. Performance of IM with load torque equal to 0 (N.m) Rotor speed and stator flux amplitude under the proposed FLC based controller method

The performance of the rotor speed and stator flux amplitude using the existing MPC approach under the same circumstances as in Fig. 9 is shown in Fig. 10a. As can be observed in Fig. 10a, the stator flux amplitude closely tracks references, whereas the rotor speed deviates from it by about 1.6%.
The effectiveness of the proposed FLC controller approach is shown in Fig. 10b. As can be seen in Fig. 10b, the rotor speed waveform is identical to that obtained using the traditional approach, and it roughly tracks the reference value. The stator flux amplitude ripple of the MPC-based DTC approach is also shown in Fig. 10b. This stator flux amplitude ripple is less than that under the conventional DTC.
Fig. 10c illustrates the electromagnetic torque comparison between the traditional DTC approach and the MPC-based DTC method. The electromagnetic torque under the traditional DTC approach is represented by the red line, whereas the electromagnetic torque under the MPC-based DTC method is shown by the blue line.

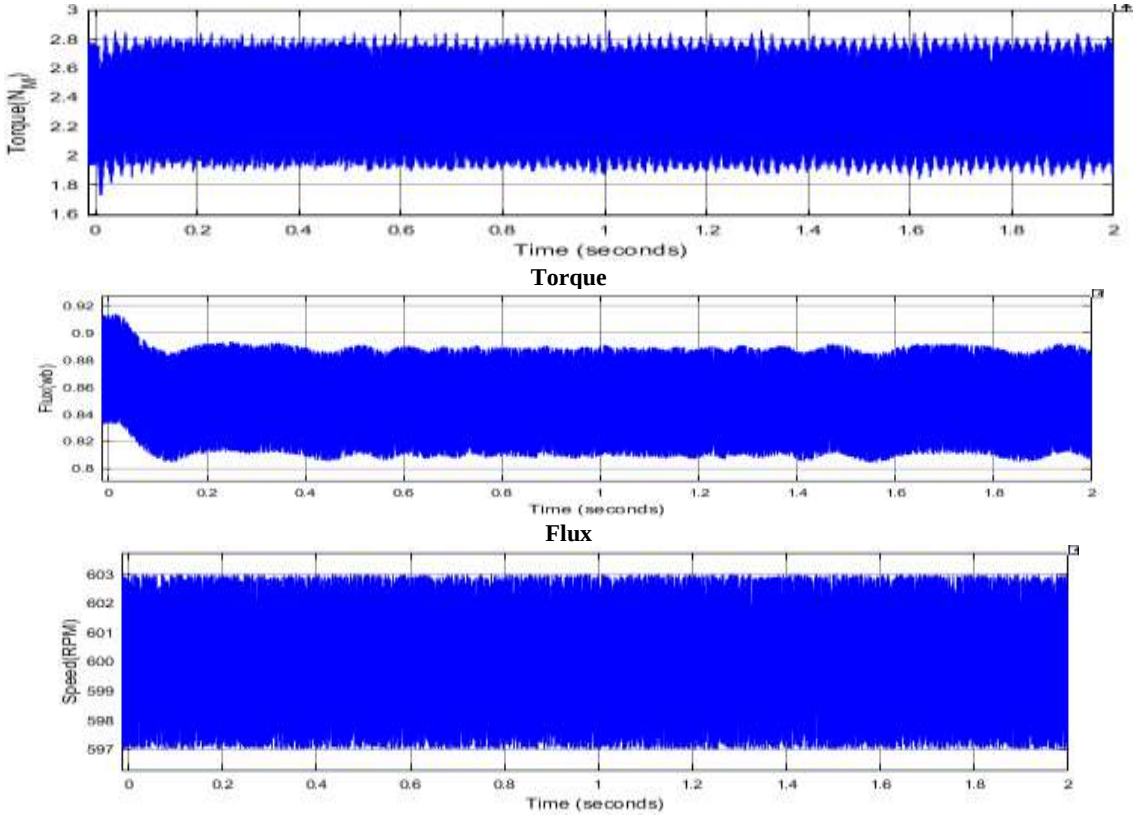

Fig. 11. Performance of IM with load torque equal to 2.5 (N.m) Rotor speed and stator flux amplitude under the proposed FLC based controller

The rotor speed and stator flux amplitude using the MPC controller approach and the suggested way are shown in Figs. 11a and 11b. The reference stator flux is 0.9 and the reference speed is 600 (r/min) (Wb). The IM's load torque is around 2.5 (N.m). The standard FLC based controller rotor speed and stator flux amplitude are shown in Fig. 11a, whereas the suggested method's rotor speed and stator flux amplitude are shown in Fig. 11b. Both techniques have comparable effects on speed tracking and flux tracking, as seen in these figures.
With a load torque of 2.5 (N.m), Fig. 11c compares the electromagnetic torque produced by using existing MPC and the proposed FLC controller approach.
Both techniques accurately track the load torque, however the torque ripple produced by the suggested technique is less. The torque ripple under the FLC controller approach is just 1.3(N.m), but the torque ripple under the traditional method is about 2(N.m).

ISSN: 2278-4632
Vol-13, Issue-02, No.01, February 2023

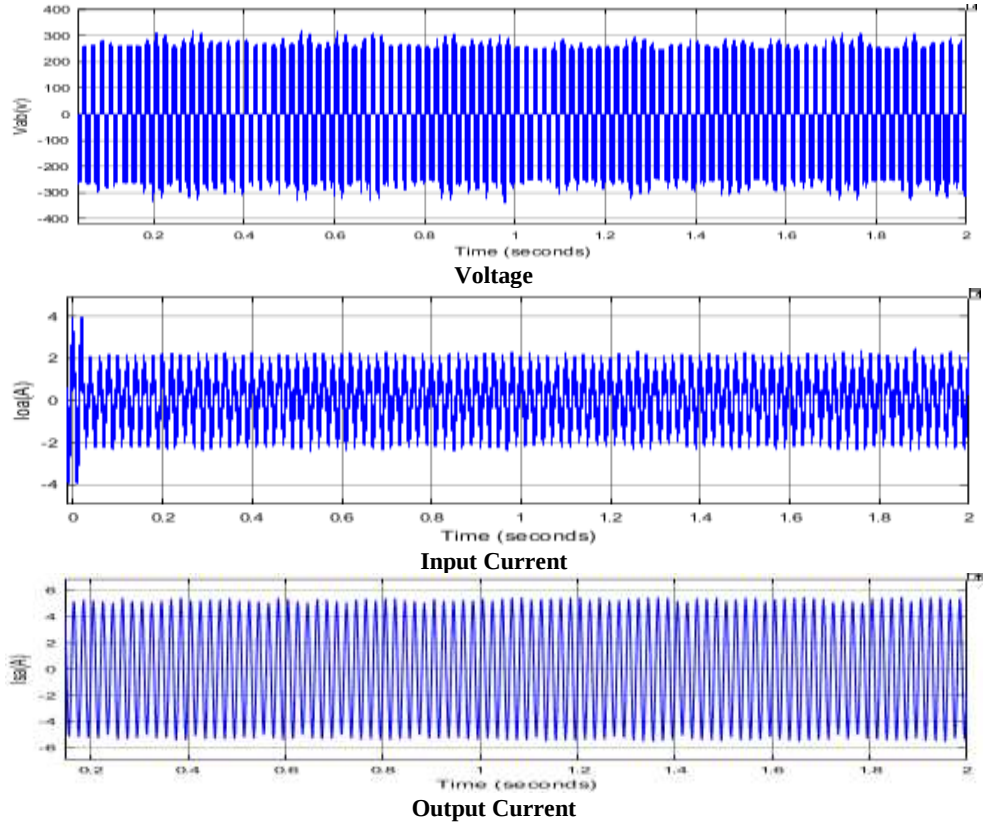

Fig. 12. Input and output waveforms of DMC with load torque equal to 2.5 (N.m) Under the proposed FLC-based controller method

In accordance with the identical conditions as in Fig. 11, Fig. 12 depicts the waveform of the output line-to-line voltage, output current, and grid current using the traditional MPC method and the FLC-based method. Regarding Fig. 12, it demonstrates that both techniques can produce sinusoidal grid current and output current with minimal distortion.

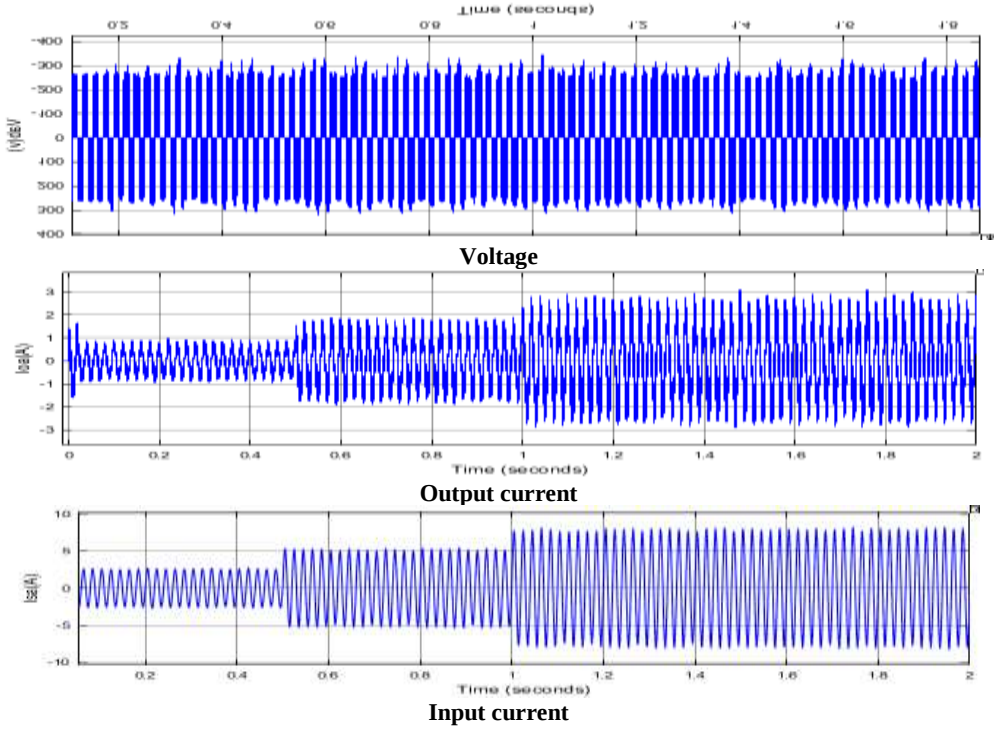

ISSN: 2278-4632
Vol-13, Issue-02, No.01, February 2023

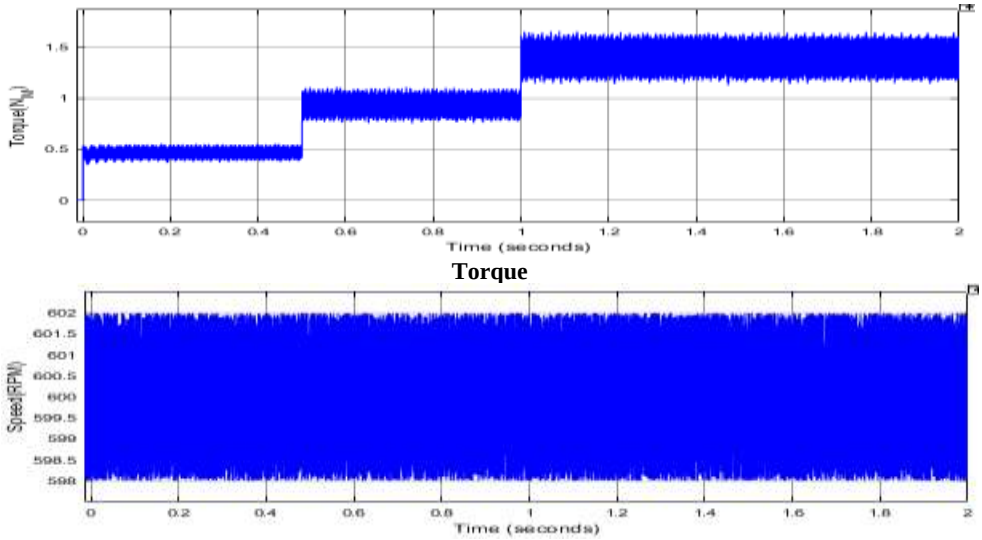

Fig. 13. Simulation results of the proposed MPC-based DTC method when the load torque changes suddenly

The simulation outcomes of the suggested strategy when the load torque varies abruptly are shown in Fig. 13. As shown in Fig. 13, the proposed FLC-based controller method inherits the FLC-based controller method's benefits, such as quick dynamic reaction. The rotor speed decreases slightly due to the rapid change in load torque, but maintains steady with no more than 0.5 seconds. The electromagnetic torque responds swiftly to changes in load torque and does the same.

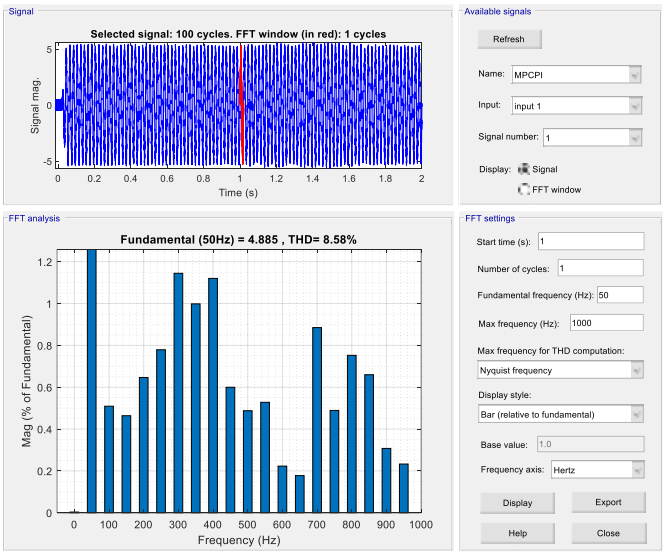

USING PI CONTROLLER

ISSN: 2278-4632
Vol-13, Issue-02, No.01, February 2023

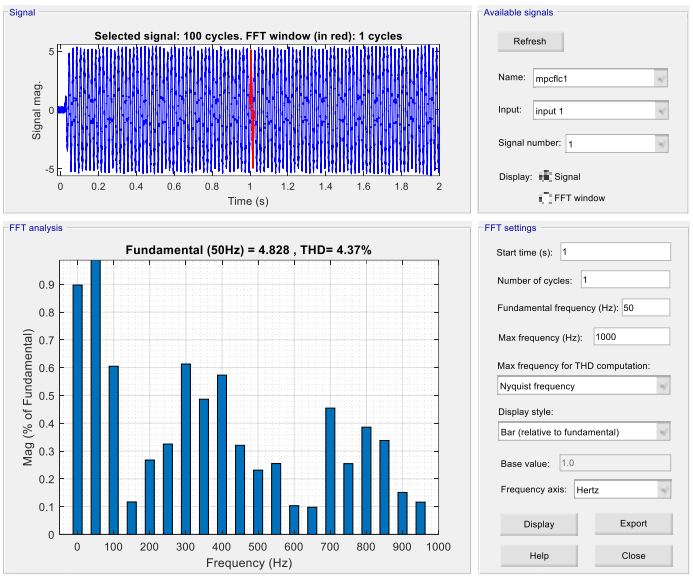

USING FUZZY LOGIC CONTROLLER

The above figure shows the THD comparision of existed PI controller proposed fuzzy logic controller

THD Comparison table

TABLE-1

parameter	MPC controller	FLC-MPC
STATOR CURRENT (Isa)	8.58%	4.37%

The above table-1 shows the THD's comparison of stator current with conventional MPC controller and proposed FLC-MPC controller. By using MPC controller the stator current THD is 8.58% and by suing FLC-MPC is 4.37%.

V CONCLUSION

In this project, An MPC-FLC based DTC method for a DMC-fed IM is presented in this paper. Six voltage vectors selected from two look-up tables along with three zero voltage vectors are utilised for prediction. The switching state that minimises the cost function is selected as the optimal switching state for the next switching period. When compared with the MPC-PI based DTC method, the proposed method evaluates the accurate values and reduces the harmonic distortion in the grid side current. The performance of the proposed method is evaluated by using MATLAB and SIMULINK software.

VI REFERENCES

[1] P. W. Wheeler, J. Rodriguez, J. C. Clare, L. Empringham, and A. Wein-stein, "Matrix converters: A technology review," IEEE Trans. Ind. Electron., vol. 49, no. 2, pp. 276–288, Apr. 2002.

[2] J. Rodriguez, M. Rivera, J. W. Kolar, and P. W. Wheeler.: "A review of control and modulation methods for matrix converters," IEEE Trans. Ind. Electron., vol. 59, no. 1, pp. 58–70, Jan. 2012.

[3] E. Yamamoto et al, "Development of MCs and its applications in industry," IEEE Trans. Ind. Electron., vol. 5, no. 1, pp. 4–12, Mar. 2011.

[4] Mohamed Basri Hazrul, Mekhilef Saad, "Experimental evaluation of model predictive current control for a modified three-level four-leg indirect matrix converter,". IET Electric Power Applications, 2017, 12 (1).

[5] P. Yao and X. Jiang, "An optimal six vector switching pattern in matrix converters for reducing harmonics and switching loss," in CSEE Journalof Power and Energy Systems, doi: 10.17775/CSEEJPES.2019.03290.

[6] W. Deng, "Maximum Voltage Transfer Ratio of Matrix Converter under DTC with Rotating Vectors," in IEEE Transactions on Power Electronics, doi: 10.1109/TPEL.2020.3033414.

ISSN: 2278-4632
Vol-13, Issue-02, No.01, February 2023

[7] D. Casadei, G. Serra, A. Tani, "The use of matrix converters in direct torque control of induction machines," IEEE Trans. Ind. Electron., vol. 4, pp. 1057-1064, 2001.
[8] Hong-Hee Lee, H. M. Nguyen, Tae-Won Chun and Won-Ho Choi, "Implementation of direct torque control method using matrix converter fed induction motor," 2007 International Forum on Strategic Technology, Ulaanbaatar, pp. 51-55, 2007.
[9] R. H. Kumar, A. Iqbal and N. C. Lenin, "Review of recent advancements of direct torque control in induction motor drives – a decade of progress," IET Power Electronics, vol. 11, no. 1, pp. 1-15, 12 1 2018.
[10] K. Lee and F. Blaabjerg, "Sensorless DTC-SVM for Induction Motor Driven by a Matrix Converter Using a Parameter Estimation Strategy," IEEE Transactions on Industrial Electronics, vol. 55, no. 2, pp. 512-521, Feb. 2008.
[11] S. Sebtahmadi, H. Pirasteh, S. Kaboli, et al, "A 12-Sector Space Vector Switching Scheme for Performance Improvement of Matrix-Converter-Based DTC of IM Drive," IEEE Trans. Power Electron, vol. 7, pp. 3804-3817, 20l5.
[12] P. Cortes, M. P. Kazmierkowski, R. M. Kennel, D. E. Quevedo, and J. Rodriguez, "Predictive control in power electronics and drives," IEEE Trans. Ind. Electron., vol. 55, no. 12, pp. 4312–4324, Dec. 2008.
[13] J. Rodriguez et al, "State of the art of finite control set model predictive control in power electronics," IEEE Trans. Ind. Informat., vol. 9, no. 2, pp. 1003–1016, May 2013.
[14] Sergio Vazquez, Jose I. Leon, Leopoldo G. Franquelo, Jose Rodriguez, et al., "Model Predictive Control: A Review of Its Applications in Power Electronics," IEEE Industrial Electronics Magazine, vol. 8, no. 1, pp. 16-31, March 2014.
[15] M. Khosravi, M. Amirbande, D. A. Khaburi, M. Rivera, J. Riveros,J. Rodriguez, A. Vahedi, and P. Wheeler, "Review of model predictive control strategies for matrix converters," IET Power Electronics, vol. 12, no. 12, pp. 3021- 3032, 2019.
[16] A. Dekka, B. Wu, V. Yaramasu, R. L. Fuentes and N. R. Zargari, "Model Predictive Control of High-Power Modular Multilevel Converters—An Overview," IEEE Journal of Emerging and Selected Topics in Power Electronics., vol. 7, no. 1, pp. 168-183, March 2019.
[17] Y. Zhang, H. Yang and B. Xia, "Model predictive torque control of induction motor drives with reduced torque ripple," IET Electric Power Applications, vol. 9, no. 9, pp. 595-604, November 2015.
[18] Muslem Uddin, Saad Mekhilef, Marizan Mubin, Marco Rivera, Jose Rodriguez. "Model Predictive Torque Ripple Reduction with Weighting Factor Optimization Fed by an Indirect Matrix Converter," Electric Power Components and Systems,vol. 42, no. 10, pp. 1059–1069, 2014.
[19] R. Vargas, J. Rodriguez, U. Ammann, and P. Wheeler, "Predictive current control of an induction machine fed by a matrix converter with reactive power control," IEEE Trans. Ind. Electron., vol. 55, no. 12, pp. 4362–4371, Dec. 2008.
[20] R. Vargas, U. Ammann, B. Hudoffsky, J. Rodriguez, and P. Wheeler, "Predictive torque control of an induction machine fed by a matrix converter with reactive input power control," IEEE Trans. Power Electron., vol. 25, no. 6, pp. 1426–1438, Jun. 2010
[21] Mohsen Siami, Davood Arab Khaburi, Marco Rivera, Jose Rodríguez, "A Computationally Efficient Lookup Table Based FCS-MPC for PMSM Drives Fed by Matrix Converters," IEEE Trans. Ind. Electron., vol. 64, no. 10, pp. 7645-7654, Oct. 2017.
[22] M. Siami, D. Arab Khaburi and J. Rodriguez, "Simplified Finite Control Set-Model Predictive Control for Matrix Converter-Fed PMSM Drives," IEEE Transactions on Power Electronics, vol. 33, no. 3, pp. 2438-2446, March 2018.
[23] T. Peng, M. Wen, Z. Li, Z. Xu, J. Yang, "An improved DTC strategy for induction motors fed by direct matrix converter," in Proc. of 2015 Chinese Automation Congress. IEEE, 2015: 1766-1771.
[24] P. Cortes, S. Kouro, B. La Rocca, R. Vargas, J. Rodriguez, J. I. Leon, S. Vazquez, and L. G. Franquelo, "Guidelines for weighting factors design in Model Predictive Control of power converters and drives," in Proc. of IEEE ICIT, pp. 1 - 7, 2009.
[25] T. Dragicevic and M. Novak, "Weighting Factor Design in Model Predictive Control of Power Electronic Converters: An Artificial Neural Network Approach," IEEE Transactions on Industrial Electronics, vol. 66, no. 11, pp. 8870 - 8880, 2019.
[26] P. L. Jansen et al, "A Physically Insightful Approach to the Design and Accuracy Assessment of Flux Observers for Field Oriented Induction Machine Drives," IEEE Trans. Ind. Appl., vol. 38, pp. 1334-1343, Sep./Oct. 2002.

ISSN: 2278-4632
Vol-13, Issue-02, No.01, February 2023

[27] Jang-Hwan Kim, Jong-Woo Choi and Seung-Ki Sul, "Novel rotor-flux observer using observer characteristic function in complex vector space for field-oriented induction motor drives," IEEE Transactions on Industry Applications, vol. 38, no. 5, pp. 1334-1343, Sept.-Oct. 2002.
[28] H. Dan, Q. Zhu, T. Peng, Y. Sun, P. Wheeler, "Preselection algorithm based on predictive control for direct matrix converter," IET Electric Power Applications, vol. 11, pp. 768-775, May 2017.